in part through a departmental grant from the National Science Foundation.

**Supplementary Material Available:** Listings of observed and calculated structure factors (34 pages). Ordering information is given on any current masthead page.

## References and Notes

(1) (a) Part 1: W. M. Maxwell, R. F. Bryan, and R. N. Grimes, *J. Am. Chem. Soc.*, preceding paper in this issue; (b) presented in part at the Third International Meeting on Boron Chemistry, Munich, Germany, July 1976.

(2) (a) W. M. Maxwell, V. R. Miller, and R. N. Grimes, *J. Am. Chem. Soc.*, **96**, 7116 (1974); (b) W. M. Maxwell, V. R. Miller, and R. N. Grimes, *Inorg. Chem.*, **15**, 1343 (1976).

(3) (a) R. Weiss, D. Freyberg, E. Sinn, and R. N. Grimes, *Inorg. Chem.*, in press; (b) R. Weiss and R. N Grimes, to be submitted for publication.

(4) W. J. Evans and M. F. Hawthorne, *J. Chem. Soc., Chem. Commun.*, 38 (1974).

(5) Throughout this article we designate the isomers of ($\eta^5$-$C_5H_5)_2Fe_2$-$(CH_3)_4C_4B_8H_8$ by Roman numerals, rather than following the usual practice[6] of distinguishing isomers by heteroatom locations [as in 1,8,5,6-$(C_5H_5)_2Co_2C_2B_5H_7$]. In the 14-vertex cages discussed here, the variation in gross geometry and the irregular nature of the polyhedra make it essentially meaningless to designate and compare isomers by heteroatom numbering. This will be true of any set of isomers lacking a common polyhedral framework.

(6) International Union of Pure and Applied Chemistry, *Pure Appl. Chem.*, **30**, 683 (1972).

(7) W. M. Maxwell, E. Sinn, and R. N. Grimes, *J. Chem. Soc., Chem. Commun.*, 389 (1976).

(8) K. Wade, *Adv. Inorg. Chem. Radiochem.*, **18**, 1 (1976).

(9) R. W. Rudolph and W. R. Pretzer, *Inorg. Chem.*, **11**, 1974 (1972).

(10) W. N. Lipscomb, "Boron Hydrides", W. A. Benjamin, New York, N.Y., 1963, p 92.

(11) For a comprehensive review of metallocarborane chemistry, see R. N. Grimes in "Organometallic Reactions and Syntheses", Vol. 6, Plenum Publishing Co., New York, N.Y., 1977, Chapter 2, pp 63–221.

(12) R. E. Williams, *Adv. Inorg. Chem. Radiochem.*, **18**, 67 (1976).

(13) J. R. Pipal and R. N. Grimes, to be submitted for publication.

(14) (a) M. K. Kaloustian, R. J. Wiersema, and M. F. Hawthorne, *J. Am. Chem. Soc.*, **94**, 6679 (1972); (b) D. F. Dustin, W. J. Evans, C. J. Jones, R. J. Wiersema, H. Gong, S. Chan, and M. F. Hawthorne, *ibid.*, **96**, 3085 (1974); (c) W. J. Evans, C. J. Jones, B. Stibr, and M. F. Hawthorne, *J. Organomet. Chem.*, **60**, C27 (1973); (d) V. R. Miller and R. N. Grimes, *J. Am. Chem. Soc.*, **97**, 4213 1975).

(15) M. Green, J. L. Spencer, F. G. A. Stone, and A. J. Welch, *J. Chem. Soc., Chem. Commun.*, 794 (1974).

(16) (a) M. Green, J. L. Spencer, F. G. A. Stone, and A. J. Welch, *J. Chem. Soc., Dalton Trans.*, 179 (1975); (b) A. J. Welch, *ibid.*, 1473 (1975); (c) W. E. Carroll, M. Green, F. G. A. Stone, and A. J. Welch, *ibid.*, 2263 (1975); (d) A. J. Welch, *ibid.*, 2270 (1975); (e) M. Green, J. A. K. Howard, J. L. Spencer, and F. G. A. Stone, *ibid.*, 2274 (1975); (e) A. J. Welch, *ibid.*, 225 (1976).

(17) D. M. P. Mingos, *J. Chem. Soc., Dalton Trans.*, 602 (1977).

(18) The new $^{11}$B NMR sign convention employed here is discussed in ref 1a, footnote 17.

(19) P. W. R. Corfield, R. J. Doedens, and J. A. Ibers, *Inorg. Chem.*, **6**, 197 (1967).

(20) D. T. Cromer and J. T. Waber, "International Tables for X-Ray Crystallography", Vol. IV, Kynoch Press, Birmingham, England, 1974.

(21) R. F. Stewart, E. R. Davidson, and W. T. Simpson, *J. Chem. Phys.*, **42**, 3175 (1965).

(22) D. T. Cromer and J. A. Ibers, "International Tables for X-Ray Crystallography", Vol. IV, Kynoch Press, Birmingham, England, 1974.

(23) Supplementary material.

---

# Ring Size Effects among Metal Complexes with Macrocyclic Ligands: Synthesis, Stereochemistry, Spectrochemistry, and Electrochemistry of Cobalt(III) Complexes with Unsubstituted, Saturated Tetraaza Macrocycles

**Yann Hung, Ludmila Y. Martin, Susan C. Jackels, A. Martin Tait, and Daryle H. Busch***

*Contribution from the Evans Chemical Laboratory, The Ohio State University, Columbus, Ohio 43210.* *Received October 10, 1976*

**Abstract:** A series of fully saturated, unsubstituted, tetraaza macrocyclic ligands, varying in ring size from 13 to 16 members, has been used to evaluate the relationships between ring size and such properties as ligand field strengths and redox potentials of complexes. Cobalt(III) complexes of the general formula $Co([13\text{-}16]aneN_4)X_n^+$ have been synthesized, where $[13]aneN_4$, $[14]aneN_4$, $[15]aneN_4$, and $[16]aneN_4$ are the saturated macrocyclic ligands and $X_n$ are $Cl_2$, $Br_2$, $(N_3)_2$, $(NCS)_2$, $(CN)_2$, or $CO_3$. Both cis and trans isomers could be prepared with $[13]aneN_4$, but only the trans geometry was found for the complexes of $[15]aneN_4$ and $[16]aneN_4$, except for the cis complexes with bidentate $CO_3^{2-}$. $[14]aneN_4$ has been studied earlier. The secondary amine groups are chiral and exhibit configurational integrity when coordinated to $Co^{3+}$. This results in the existence of configurational isomers of both *trans*-$Co([15]aneN_4)Cl_2^+$ and *trans*-$Co([16]aneN_4)Cl_2^+$, which have been separated and characterized. Strain energy calculations, $^{13}$C NMR spectra, and chemical properties are used to deduce the detailed structures of these configurational isomers. The spectrochemical consequences of ring size are revealed in the variations of the ligand field parameters $Dq^{xy}$ (due to macrocyclic ligand field) and $Dq^z$ (due to monodentate axial ligands). $Dq^{xy}$ varies with the macrocycles in the order $13 > 14 > 15 > 16$. The ligand $[14]aneN_4$ exhibits a $Dq^{xy}$ value that is normal for saturated amines—that ring size fits $Co^{3+}$ best. The smaller ring $[13]aneN_4$ exerts a constrictive effect on the metal ion because of excess strain energy. This produces an enhancement in $Dq^{xy}$. The large rings, $[15]aneN_4$ and $[16]aneN_4$, are caused by strain energy effects to exert a dilative effect on the $Co^{3+}$–N linkages, thereby producing a diminished ligand field ($Dq^{xy}$). $Dq^{xy}$ also differs among configurational isomers. The range of $Dq^{xy}$ spanned with the ligands $[13\text{-}16]aneN_4$ is 511 cm$^{-1}$ for the trans isomers, while $Dq^{av}$ only ranges over 144 cm$^{-1}$ for the cis isomers (carbonates). The redox potentials for the *trans*-$Cl_2Co^{3+}$ complexes follow the trend in strain energy rather than the trend in $Dq^{xy}$. Thus $Co^{3+}$ is most stable in *trans*-$Co([14]aneN_4)Cl_2^+$ and least stable in *trans*-$Co([16]aneN_4)Cl_2^+$. The geometric constraints that relate to the fit between a metal ion and a given size of macrocyclic ligand provide some of the most distinctive relationships among these substances.

The occurrence of macrocyclic ligands in the structures of a number of the most prominent biologically important, natural complexes strongly implies that there are significant advantages in the macrocyclic ligand structure. The importance of ring size is equally apparent in the occurrence of a 16-membered inner ring in the porphyrin ligand of the heme

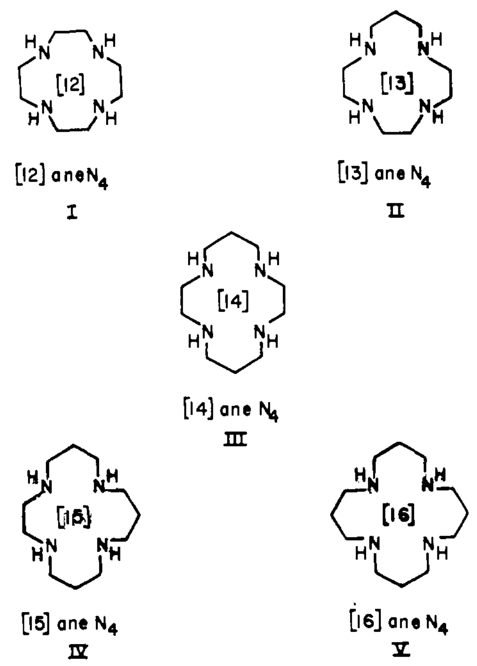

**Figure 1.** Homologous, fully saturated tetraaza macrocyclic ligands.

proteins and a 15-membered inner ring in the corrin ligand of vitamin $B_{12}$. Their cyclic natures are but one facet of the highly specialized structures occurring among these natural products. The presence of fused rings, ligand charges, and extensive chromophoric $\pi$-electron systems makes it impossible to discern the extent to which the specialized properties of such complexes derive from the fact that the ligands are macrocycles. In order to learn the special ligating qualities that derive from the cyclic nature of macrocyclic ligands, it is necessary to work with synthetic structures. The structural parameter that is most obviously characteristic of the macrocyclic structures of ligands of this class is just ring size. While many studies have been carried out on metal complexes of macrocyclic ligands,[1] it is only relatively recently that synthetic developments in these laboratories[2,3] have provided the ideal ligands for the study of this important parameter—ring size. The prototypic ligand for the entire realm of coordination chemistry is the saturated amine, such as ammonia or ethylenediamine. Appropriately then, the prototypic macrocycles are the polyazacycloalkanes, of which the tetraazacycloalkanes of Figure 1 are the simplest rings related to the porphyrin and corrin rings (by the same number of nitrogen donors and their cyclic natures). Whereas [12]aneN$_4$ and [14]aneN$_4$ (also called cyclam) have long been known, the three remaining ligands were first synthesized during the course of the on-going investigations of which the work summarized in the present report is part.

As a result of early investigations, it was suggested that 14-membered macrocycles exert abnormally large ligand fields because of a constrictive effect exerted on the metal ion by the ligand.[4] Recent studies on iron(II)[2] and nickel(II)[3] have provided substantial support for this point of view. However, the studies reported here, which are based on cobalt(III) complexes, most effectively demonstrate the nuances of this important phenomenon. A preliminary report has appeared.[5] The use of cobalt(III) was, of course, strongly indicated by the immense classical literature on the subject and the high probability of meaningful electronic spectral results.[6] The complexes of [14]aneN$_4$ with nickel(II)[7] and cobalt(III)[8,9] have been prepared and characterized, as have complexes of [12]aneN$_4$.[10] The latter has been found to form only *cis*-diacidotetramine complexes with cobalt(III). This results from the fact that [12]aneN$_4$ is too small a ring to encompass the metal ions of the transition elements. We report here the preparation and characterization of appropriate cobalt(III) complexes with the new ligands [13]aneN$_4$, [15]aneN$_4$, and [16]aneN$_4$. The usual physical measurements are used to characterize the new complexes. The synthetic studies have yielded unusual configurational isomers for *trans*-Co([15]aneN$_4$)Cl$_2$$^+$ and *trans*-Co([16]aneN$_4$)Cl$_2$$^+$. The detailed structures of these isomers have been deduced on the basis of $^{13}$C NMR spectra, theoretical strain energy calculations, and constraining chemical properties. Electronic spectra of these most meaningful complexes are then used to deduce spectrochemical parameters and these are discussed in terms of the strain energy model for the complexes. The results of electrochemical measurements are considered in the same context.

## Results and Discussion

**Syntheses and Characterization.** Complexes of [13]aneN$_4$, [15]aneN$_4$, and [16]aneN$_4$ of the formula [Co([13–16]aneN$_4$)X$_n$]$^+$ have been synthesized, where X$_n$ is Cl$_2$, Br$_2$, (N$_3$)$_2$, (NCS)$_2$, (CN)$_2$, or CO$_3$. Salts of the complexes were obtained as perchlorates, nitrates, or chlorides. All of the compounds give satisfactory elemental analyses (Table I). Conductivity measurements (Table I) indicate that the compounds are 1:1 electrolytes.[11] The compounds are diamagnetic with residual magnetic moments of ~0.6 $\mu_B$, as expected for low-spin six-coordinate cobalt(III) derivatives.

**Cis Complexes.** The series of *cis*-carbonato complexes with macrocyclic ligands [13–16]aneN$_4$ was prepared by reaction of the appropriate *trans*-dichloro complex with lithium carbonate in water. Poon[12] has shown that the number and position of the infrared bands in the CH$_2$ rocking region (800–910 cm$^{-1}$) can be used to distinguish between cis and trans isomers in the case of [Co([14]aneN$_4$)X$_2$]$^+$. In general, the cis compounds exhibit five or more bands between 800 and 910 cm$^{-1}$, while the trans compounds have two bands close to 900 cm$^{-1}$ and one close to 800 cm$^{-1}$, the intensities being somewhat weaker in the case of the cis complexes. The infrared bands of the carbonato derivatives of Co[13–16]aneN$_4$ in the CH$_2$ rocking region (Table II) agree in number and intensity with their formulation as cis complexes. The N–H stretching absorption bands for the complexes are listed in Table III. Each cis complex displays more than one $\nu_{N-H}$ due to the low (maximum $C_{2v}$) symmetry of the molecule. The CO$_3$$^{2-}$ ligand absorption bands were assigned (Table III) following the precedents given by Nakamoto[13] for bidentate carbonato complexes.

The electronic spectra of low-spin six-coordinate cobalt(III) complexes usually exhibit two d–d transitions, $^1T_{1g} \leftarrow {}^1A_{1g}$ and $^1T_{2g} \leftarrow {}^1A_{1g}$.[14] The average ligand field strength $Dq^{av}$ (Table IV) can be calculated from the equation

$$10Dq^{av} = \nu_{{}^1T_{1g}\leftarrow{}^1A_{1g}} + C \qquad (1)$$

where $C$ is assumed to have the value[6] 3800 cm$^{-1}$. For the *cis*-carbonato complex series, the positions of the bands vary only slightly with changes in macrocyclic ring size, the total range being only 144 cm$^{-1}$ for the $Dq^{av}$ values. The $Dq^{av}$ values are in the order [13]aneN$_4$ > [14]aneN$_4$ > [15]aneN$_4$ > [12]aneN$_4$ > [16]aneN$_4$ and some of the differences are indeed small. Thus, the energies of the electronic transitions of the carbonato complexes show little sensitivity toward ring size.

Both cis and trans isomers of the dibromo and dichloro complexes were obtained for the 13-membered macrocyclic ligand as confirmed by the numbers and positions[12] of the infrared bands in the CH$_2$ rocking region (Table II) and by the electronic spectra[14] (Table IV). Both cis and trans isomers were isolated[8,9] for Co([14]aneN$_4$)X$_n$$^+$, whereas only the trans isomers were isolated for Co([15]aneN$_4$)X$_n$$^+$ and Co([16]-

**Table I.** Analytical Data and the Molar Conductivities[a] for the New Complexes

| Compd | % C Calcd | % C Found | % H Calcd | % H Found | % N Calcd | % N Found | Λ, $ohm^{-1}\ cm^2\ mol^{-1}$; solvent |
|---|---|---|---|---|---|---|---|
| *trans*-$[Co([13]aneN_4)Cl_2]Cl$ | 30.75 | 30.52 | 6.31 | 6.24 | 15.94 | 15.66 | 77 methanol |
| *cis*-$[Co([13]aneN_4)Cl_2]Cl$ | 30.75 | 30.70 | 6.31 | 6.85 | 15.94 | 15.70 | 77 methanol |
| *trans*-$[Co([13]aneN_4)Br_2]ClO_4$ | 21.42 | 21.89 | 4.36 | 4.42 | 11.11 | 11.43 | 91 methanol |
| *cis*-$[Co([13]aneN_4)Br_2]ClO_4$ | 21.42 | 21.96 | 4.36 | 4.45 | 11.11 | 11.32 | 85 methanol |
| *trans*-$[Co([13]aneN_4)(N_3)_2]ClO_4$ | 25.21 | 25.89 | 5.13 | 5.13 | 32.68 | 33.34 | 110 methanol |
| *trans*-$[Co([13]aneN_4)(NCS)_2]ClO_4$ | 28.67 | 28.63 | 4.78 | 4.83 | 18.25 | 17.98 | 88 methanol |
| *trans*-$[Co([13]aneN_4)(NO_2)_2]ClO_4$ | 24.75 | 24.95 | 5.04 | 5.05 | 19.25 | 19.18 | 87 water |
| *trans*-$[Co([13]aneN_4)(CN)_2]ClO_4$ | 33.30 | 33.47 | 5.55 | 5.52 | 21.19 | 21.00 | 88 water |
| *trans*-$[Co([14]aneN_4)Cl_2]Cl \cdot H_2O$ | 31.64 | 31.57 | 5.84 | 6.44 | 14.76 | 15.09 | 74 methanol |
| *trans*-(I)-$[15]aneN_4)Cl_2]NO_3$ | 32.53 | 31.98 | 6.45 | 6.55 | 17.24 | 17.37 | 84 methanol |
| *trans*-(II)-$[Co([15]aneN_4)Cl_2]Cl$ | 34.80 | 34.38 | 6.90 | 7.24 | 14.76 | 14.41 | 81 nitromethane |
| *trans*-$[Co([15]aneN_4)Br_2]ClO_4$ | 24.80 | 25.03 | 4.89 | 4.89 | 10.52 | 10.58 | 100 methanol |
| *trans*-$[Co([15]aneN_4)(N_3)_2]ClO_4$ | 28.92 | 29.04 | 5.70 | 5.70 | 30.67 | 30.17 | 75 methanol |
| *trans*-$[Co([15]aneN_4)(NCS)_2]ClO_4$ | 31.93 | 31.61 | 5.32 | 5.20 | 17.20 | 17.32 | 92 methanol |
| *trans*-$[Co([15]aneN_4)(NO_2)_2]ClO_4$ | 28.42 | 28.60 | 5.60 | 5.35 | 18.09 | 18.03 | 110 methanol |
| *trans*-$[Co([15]aneN_4)(CN)_2]ClO_4$ | 36.76 | 36.53 | 6.13 | 5.88 | 19.79 | 19.85 | 79 methanol |
| *trans*-$[Co([16]aneN_4)Br_2]ClO_4$ | 26.36 | 26.55 | 5.13 | 5.02 | 10.25 | 10.43 | 89 methanol |
| *trans*-(I)-$[Co([16]aneN_4)Cl_2]ClO_4$ | 31.48 | 31.28 | 6.12 | 5.92 | 12.24 | 12.04 | 132 acetonitrile |
| *trans*-(II)-$[Co([16]aneN_4)Cl_2]ClO_4$ | 31.48 | 31.40 | 6.12 | 6.20 | 12.24 | 12.21 | 145 acetonitrile |
| *trans*-$[Co([16]aneN_4)(N_3)_2]ClO_4$ | 30.61 | 30.88 | 5.95 | 5.89 | 29.76 | 29.87 | 90 methanol |
| *trans*-$[Co([16]aneN_4)(NCS)_2]ClO_4$ | 33.44 | 33.70 | 5.57 | 5.70 | 16.72 | 16.66 | 91 methanol |
| *trans*-$[Co([16]aneN_4)(NO_2)_2]ClO_4$ | 30.10 | 30.25 | 5.85 | 6.00 | 17.56 | 17.26 | 103 water |
| *trans*-$[Co([16]aneN_4)(CN)_2]ClO_4$ | 38.32 | 38.35 | 6.39 | 6.55 | 19.16 | 18.72 | 89 methanol |
| *cis*-$[Co([16]aneN_4)(CO_3)]ClO_4$ | 29.68 | 29.61 | 5.48 | 5.11 | 13.84 | 13.66 | 81 water |
| *cis*-$[Co([15]aneN_4)(CO_3)]ClO_4 \cdot 3/2H_2O$ | 31.35 | 31.45 | 6.36 | 6.18 | 12.19 | 12.15 | 90 water |
| *cis*-$[Co([16]aneN_4)(CO_3)]ClO_4$ | 35.11 | 34.74 | 5.89 | 6.43 | 12.60 | 12.50 | 95 water |

[a] $\sim 10^{-3}$ M solution at room temperature.

**Table II.** Infrared Spectral Bands in the $CH_2$ Rocking Region for $[Co([13\text{–}16]aneN_4)X_2]ClO_4$ ($cm^{-1}$)

| Complex | $CH_2$ rocking region |
|---|---|
| *cis*-$[Co([13]aneN_4)CO_3]ClO_4$ | 813 w, 820 w, 828 s,[a] 847 m, 866 w, 873 sh, 899 w |
| *cis*-$[Co([15]aneN_4)CO_3]ClO_4$ | 808 w, 821 w, 827 s,[a] 845 w, 872 m, 890 w, 905 w |
| *cis*-$[Co([16]aneN_4)CO_3]ClO_4$ | 789 w, 826 w,[a] 889 w, 903 m |
| *cis*-$[Co([13]aneN_4)Cl_2]ClO_4$ | 899 w, 875 w, 867 w, 847 w, 831 w |
| *cis*-$[Co([13]aneN_4)Br_2]ClO_4$ | 901 w, 885 w, 873 w, 856 w, 820 w |
| *trans*-$[Co([13]aneN_4)Br_2]ClO_4$ | 899 m, 875 s, 824 m |
| *trans*-$[Co([13]aneN_4)Cl_2]ClO_4$ | 901 s, 877 s, 822 m |
| *trans*-$[Co([13]aneN_4)(N_3)_2]ClO_4$ | 894 w, 876 m, 847 m |
| *trans*-$[Co([13]aneN_4)(NCS)_2]ClO_4$ | 901 m, 885 s, 854 ($\nu$CS), 829 w |
| *trans*-$[Co([13]aneN_4)(NO_2)_2]ClO_4$ | 901 m, 872 m, 826 ($\delta$ONO), 818 s |
| *trans*-$[Co([13]aneN_4)(CN)_2]ClO_4$ | 899 m, 877 s, 814 |
| *trans*-$[Co([15]aneN_4)Br_2]ClO_4$ | 899 s, 855 m, 833 w |
| *trans*-(I)-$[Co([15]aneN_4)Cl_2]NO_3$ | 892 m, 882 w, 837 w, 813 w |
| *trans*-(II)-$[Co([15]aneN_4)Cl_2]NO_3$ | 875 m, 837 w, 831 w, 815 w |
| *trans*-$[Co([15]aneN_4)(N_3)_2]ClO_4$ | 901 s, 855 m, 826 w |
| *trans*-$[Co([15]aneN_4)(NCS)_2]ClO_4$ | 901 m, 893 w, 855 ($\nu$CS), 826 w |
| *trans*-$[Co([15]aneN_4)(NO_2)_2]ClO_4$ | 893 m, 880 w, 853 w, 826 ($\delta$ONO) |
| *trans*-$[Co([15]aneN_4)(CN)_2]ClO_4$ | 901 m, 855 w, 826 w ($\delta$ONO) |
| *trans*-$[Co([16]aneN_4)Br_2]ClO_4$ | 901 m, 875 m, 830 m |
| *trans*-(I)-$[Co([16]aneN_4)Cl_2]ClO_4$ | 901 m, 870 m, 845 w |
| *trans*-(II)-$[Co([16]aneN_4)Cl_2]ClO_4$ | 893 m, 873 (sh), 806 m |
| *trans*-$[Co([16]aneN_4)(N_3)_2]ClO_4$ | 901 m, 895 m |
| *trans*-$[Co([16]aneN_4)(NCS)_2]ClO_4$ | 901 m, 858 ($\nu$CS), 810 w |
| *trans*-$[Co([16]aneN_4)(NO_2)_2]ClO_4$ | 901 m, 893 m, 855 w, 826 |
| *trans*-$[Co([16]aneN_4)(CN)_2]ClO_4$ | 899 m, 877 w, 810 w |

[a] Overlaps with the $CO_3^{2-}$ absorption.

$aneN_4)X_n^+$ (see below). It is interesting to note that strain energy calculations have shown that the 14-membered macrocycle best fits the cobalt(III) ion in the *trans*-diacido-tetramine structures (see below). The 13-membered and 12-membered macrocycles, which have smaller ring sizes, would be expected to have greater tendencies to adopt folded conformations. The 15- and 16-membered macrocycles may incur steric crowding in the cis conformation and therefore be more disposed toward trans conformations. Thus, the following qualitative correlation between ring size and isolated products can be made: $[12]aneN_4$, cis only; $[13,14]aneN_4$, cis and trans; and $[15,16]aneN_4$, trans only.

**Trans Complexes.** The $[13]aneN_4$ and $[15]aneN_4$ complexes were prepared by mixing methanol solutions of the ligand and a cobalt(II) salt, followed by addition of excess HCl or HBr and air oxidation. However, treatment of methanolic

Table III. Selected Infrared Spectral Bands[a] for $[Co([13-16]aneN_4)X_2]ClO_4$

| Complex | $\nu_{(NH)}$, $cm^{-1}$ | $\nu_{(X)}$, $cm^{-1}$ | Assignment |
|---|---|---|---|
| *cis*-$[Co([13]aneN_4)CO_3]ClO_4$ | 3257 s,sp, 3205 s,br | 1653 s,sp, 1605br 831 m, 752 m, 676 m | $\nu_{(CO)}$ |
| *cis*-$[Co([15]aneN_4)CO_3]ClO_4$ | 3255 s,sp, 3200 br | 1662 s,sp, 1621br 828 m, 750 m, 676 m | $\nu_{(CO)}$ |
| *cis*-$[Co([16]aneN_4)CO_3]ClO_4$ | 3257 sh, 3236 s,sp, 3165 s | 1656 s,sp, 1613br 828 m, 752 m, 672 m | $\nu_{(CO)}$ |
| *cis*-$[Co([13]aneN_4)Br_2]ClO_4$ | 3268 s,sp, 3175 s, 3106 w | | |
| *cis*-$[Co([13]aneN_4)Cl_2]ClO_4$ | 3271 s,sp, 3177 s,br | | |
| *trans*-$[Co([13]aneN_4)Br_2]ClO_4$ | 3228 s,sp, 3219 s,sp | | |
| *trans*-$[Co([13]aneN_4)Cl_2]ClO_4$ | 3234 s | | |
| *trans*-$[Co([13]aneN_4)(N_3)_2]ClO_4$ | 3248 s,br | 2050 vs,br, 1292 m | $\nu_{(NN)}$ |
| *trans*-$[Co([13]aneN_4)(NCS)_2]ClO_4$ | 3315 sh, 3219 s,br | 2120 vs, 2063 sh, 855 | $\nu_{(NC)}$, $\nu_{(CS)}$ |
| *trans*-$[Co([13]aneN_4)(NO_2)_2]ClO_4$ | 3226 br | 1402 m, 1323 s, 826 m | $\nu_{as}(NO_2)$,<br>$\nu_{sy}(NO_2)$,<br>$\delta_{(ONO)}$ |
| *trans*-$[Co([13]aneN_4)(CN)_2]ClO_4$ | 3260 s,sp, 3187 s | 2136 s,sp | $\nu_{(CN)}$ |
| *trans*-$[Co([15]aneN_4)Br_2]ClO_4$ | 3220 s,sp | | |
| *trans*-(I)-$[Co([15]aneN_4)Cl_2[NO_3$ | 3200 s,sp | | |
| *trans*-(II)-$[Co([15]aneN_4)Cl_2]NO_3$ | 3160 s,sp | | |
| *trans*-$[Co([15]aneN_4)(N_3)_2]ClO_4$ | 3238 s | 2040 vs, 1291 s | $\nu_{(NN)}$ |
| *trans*-$[Co([15]aneN_4)(NCS)_2]ClO_4$ | 3225 sh, 3175 s,br | 2109 vs, 855 | $\nu_{(NC)}$, $\nu_{(CS)}$ |
| *trans*-$[Co([15]aneN_4)(NO_2)_2]ClO_4$ | 3226 m,sp, 3195 s,sp | 1404 s, 1309 vs, 826 s | $\nu_{as}(NO_2)$,<br>$\nu_{sy}(NO_2)$,<br>$\delta_{(ONO)}$ |
| *trans*-$[Co([15]aneN_4)(CN)_2]ClO_4$ | 3318 sh, 3241 s,br | 2144 s,sp | $\nu_{(CN)}$ |
| *trans*-$[Co([16]aneN_4)Br_2]ClO_4$ | 3230 s,sp, 3147 w | | |
| *trans*-(I)-$[Co([16]aneN_4)Cl_2]ClO_4$ | 3236 s, 3175 s,sp | | |
| *trans*-(II)-$[Co([16]aneN_4)Cl_2]ClO_4$ | 3247, 3174 s,sp | | |
| *trans*-$[Co([16]aneN_4)(N_3)_2]ClO_4$ | 3271 s | 2056 s,br, 2041 sh | $\nu_{(NN)}$ |
| *trans*-$[Co([16]aneN_4)(NCS)_2]ClO_4$ | 3257 s, 3143 sh | 2102 s,br, 855 m | $\nu_{(NC)}$, $\nu_{(CS)}$ |
| *trans*-$[Co([16]aneN_4)(NO_2)_2]ClO_4$ | 3238 s,sp | 1408 vs, 1312 vs, 826 s,sp | $\nu_{as}(NO_2)$,<br>$\nu_{sy}(NO_2)$,<br>$\delta_{(ONO)}$ |
| *trans*-$[Co([16]aneN_4)(CN)_2]ClO_4$ | 3289 s,sp, 3197 vs,sp | 2141 s,sp | $\nu_{(CN)}$ |

[a] Nujol mull method, abbreviations: s = strong, sp = sharp, sh = shoulder, vs = very strong, br = broad, m = medium, w = weak.

Table IV. Electronic Spectral Data for *cis*-$[Co([12-16]aneN_4)X]^+$ Complexes[a]

| | Band max, $\mu m^{-1}$ | | |
|---|---|---|---|
| Complex | $^1T_{1g} \leftarrow {}^1A_{1g}$ | $^1T_{2g} \leftarrow {}^1A_{1g}$ | $Dq^{av}$, $cm^{-1}$ |
| $[Co([12]aneN_4)CO_3]^+$ [c] | 1.887 (280) | 2.717 (210) | 2267 |
| $[Co([13]aneN_4)CO_3]^+$ | 1.996 (178) | 2.809 (133) | 2376 |
| $[Co([14]aneN_4)CO_3]^+$ | 1.923 (154) | 2.740 (140) | 2303 |
| $[Co([15]aneN_4)CO_3]^+$ | 1.894 (138) | 2.732 (182) | 2274 |
| $[Co([16]aneN_4)CO_3]^+$ | 1.852 (146) | 2.667 (197) | 2232 |
| $[Co([13]aneN_4)Cl_2]^+$ [b] | 1.852 (124) | Masked | 2232 |

[a] In water. [b] In methanol. [c] Reference 10.

$[16]aneN_4$–cobalt(II) solutions with HCl or HBr led to destruction of the complex as evidenced by formation of the protonated ligand. Therefore, the preparation of Co[16]aneN$_4$ complexes was carried out in $CHCl_3$ using bromine as the oxidant. Only three infrared bands (or fewer in the cases of some 16-membered ring derivatives) were observed in the $CH_2$ rocking region (Table II), suggesting the trans geometry.[12] Two configurational (N-H) isomers of *trans*-$Co([15]aneN_4)Cl_2^+$ and *trans*-$Co([16]aneN_4)Cl_2^+$ were separated and characterized and will be discussed below. Both the $NCS^-$ and the $NO_2^-$ derivatives are N-bonded[15,16] as indicated from the infrared spectral data (Table III).

The electronic spectra are reported in Table V. The energy diagram for a low-spin $d^6$ ion in $O_h$ and $D_{4h}$ symmetry is shown in Figure 2. Two spin-allowed d-d transitions are expected for true octahedral complexes ($^1T_{1g} \leftarrow {}^1A_{1g}$ and $^1T_{2g} \leftarrow {}^1A_{1g}$); however, when the symmetry is lowered to $D_{4h}$ each of the octahedral states ($^1T_{1g}$ and $^1T_{2g}$) splits into two states. Hence, more than two bands are expected. Usually, three bands are observed; i.e., $^1E_g{}^a \leftarrow {}^1A_{1g}$, $^1A_{2g} \leftarrow {}^1A_{1g}$, and $(^1E_g{}^b + {}^1B_{2g}) \leftarrow {}^1A_{1g}$. The ligand field strength parameters $Dq^{xy}$ and $Dq^z$ can be calculated[6] according to the following equations.

$$10Dq^{xy} = \nu_{^1A_{2g} \leftarrow {}^1A_{1g}} + C \qquad (2)$$

$$Dt = -(4/35)(\nu_{^1E_g{}^a \leftarrow {}^1A_{1g}} - \nu_{^1A_{2g} \leftarrow {}^1A_{1g}}) \qquad (3)$$

$$Dq^z = Dq^{xy} - (7/4)Dt \qquad (4)$$

$C$ is roughly constant and is usually assumed[6] to have the value 3800 $cm^{-1}$. $Dq^{xy}$ is the ligand field splitting parameter in the $xy$ plane (macrocycle) and $Dq^z$ is that on the $z$ axis (axial ligands). In order to apply the above equations to the spectra of $[13-16]aneN_4$ complexes $D_{4h}$ symmetry must be assumed. This amounts to assuming that the four macrocyclic nitrogen atoms are coordinated in an ideal square planar array and impose equivalent ligand fields on the metal ion. This assumption obviously does not hold in all of the cases being considered here; however, many of the derivatives do display the three predicted bands, thereby indicating the close approximation to $D_{4h}$ symmetry. We have chosen to apply the $D_{4h}$ model for this reason and also because other low-spin Co(III) macrocyclic systems lacking true $D_{4h}$ symmetry have been usefully treated assuming the $D_{4h}$ model.[17]

Spectral band assignments for the $Co([13-16]aneN_4)X_2^+$ derivatives are shown in Table V. It should be noted that in the case of the *trans*-$Co([15]aneN_4)Cl_2^+$ and *trans*-$Co([16]aneN_4)Cl_2^+$ complexes configurational isomers have been separated and characterized (see below). The derivatives of other axial ligands may exist as mixtures of two or more (N-H) configurational isomers. For this reason only the series of *trans*-dichloro complexes is discussed in detail.

For the *trans*-dichloro derivatives, as the size of the macrocyclic ring increases (13 → 16) the $^1A_{2g}$ band moves to lower

Table V. Electronic Spectral Band Assignments for *trans*-[Co([13-16]aneN$_4$)X$_2$]ClO$_4$ Complexes (in $\mu$m$^{-1}$)[a,b]

| Complex | $^1E_g{}^a \leftarrow {}^1A_{1g}$ $\nu$ ($\epsilon_M$) | $^1A_{2g} \leftarrow {}^1A_{1g}$ $\nu$ ($\epsilon_M$) | $^1B_{2g} + {}^1E_g{}^b \leftarrow {}^1A_{1g}$ $\nu$ ($\epsilon_M$) |
|---|---|---|---|
| [Co([13]aneN$_4$)Cl$_2$]ClO$_4$ | 1.667 (33) | 2.370 (144) | |
| [Co([14]aneN$_4$)Cl$_2$]Cl·H$_2$O | 1.620 (35) | 2.182 (24) | 2.586 (56) |
| (I)-[Co([15]aneN$_4$)Cl$_2$]NO$_3$ | 1.527 (40) | 1.923 (69) | 2.370 (106) |
| (II)-[Co([15]aneN$_4$)Cl$_2$]Cl | 1.563 (27) | 2.041 (38) | 2.410 (62) |
| (I)-[Co([16]aneN$_4$)Cl$_2$]ClO$_4$ | 1.473 (57) | 1.869 (34) | 2.326 (99) |
| (II)-[Co([16]aneN$_4$)Cl$_2$]ClO$_4$ | 1.511 (41) | 1.961 (35) | 2.387 (76) |
| [Co([13]aneN$_4$)Br$_2$]ClO$_4$ | 1.539 (22) | 2.222 (sh) | |
| [Co([15]aneN$_4$)Br$_2$]ClO$_4$ | 1.439 (43) | 1.980 (sh) | |
| [Co([16]aneN$_4$)Br$_2$]ClO$_4$ | 1.379 (38) | 1.852 (sh) | |
| [Co([13]aneN$_4$)(N$_3$)$_2$]ClO$_4$ | 1.869 (244) | | |
| [Co([14]aneN$_4$)(N$_3$)$_2$]ClO$_4$[c] | 1.740 (430) | | |
| [Co([15]aneN$_4$)(N$_3$)$_2$]ClO$_4$ | 1.689 (369) | | |
| [Co([16]aneN$_4$)N$_3$)$_2$]ClO$_4$ | 1.626 (346) | | |
| [Co([13]aneN$_4$)(NCS)$_2$]ClO$_4$ | 1.961 (397) | | |
| [Co([14]aneN$_4$)(NCS)$_2$]NCS[c] | 1.920 (267) | | |
| [Co([15]aneN$_4$)(NCS)$_2$]ClO$_4$ | 1.795 (356) | | |
| [Co([16]aneN$_4$)(NCS)$_2$]ClO$_4$ | 1.770 (311) | | |
| [Co([13]aneN$_4$)(NO$_2$)$_2$]ClO$_4$ | 2.198 (297) | | |
| [Co([14]aneN$_4$)(NO$_2$)$_2$]ClO$_4$[c] | 2.170 (189) | | |
| [Co([15]aneN$_4$)(NO$_2$)$_2$]ClO$_4$ | 2.151 (209) | | |
| [Co([16]aneN$_4$)(NO$_2$)$_2$]ClO$_4$ | 2.128 (266) | | |
| [Co([13]aneN$_4$)(CN)$_2$]ClO$_4$ | 2.564[d] | 2.299[d] | 3.279 (135) |
| [Co([15]aneN$_4$)(CN)$_2$]ClO$_4$ | 2.299 (93) | 1.980 (sh) | 3.125 (sh) |
| [Co([16]aneN$_4$)(CN)$_2$]ClO$_4$ | 2.247 (77) | 1.923 (sh) | 2.857 (sh) |

[a] Spectra of Cl$^-$ derivatives in methanol, all others in acetonitrile. [b] Band positions and extinction coefficients derived from Gaussian analysis of observed spectrum. [c] Spectral transitions for [Co([14)aneN$_4$)X$_2$]$^+$ complexes obtained from ref 7. [d] Gaussian components of spectral band centered at 2.41 $\mu$m$^{-1}$.

Table VI. Ligand Field Parameters for *trans*-[Co([13-16]aneN$_4$)Cl$_2$]$^+$ Complexes (cm$^{-1}$)

| Complex | Ligand field parameters | | |
|---|---|---|---|
| | $Dq^{xy}$ | $Dq^z$ | $Dt$ |
| [Co([13]aneN$_4$)Cl$_2$]ClO$_4$ | 2750 | 1345 | 803 |
| [Co([14]aneN$_4$)Cl$_2$]Cl·H$_2$O | 2562 | 1437 | 642 |
| (II)-[Co([15]aneN$_4$)Cl$_2$]Cl | 2421 | 1465 | 546 |
| (I)-[Co([15]aneN$_4$)Cl$_2$]NO$_3$ | 2303 | 1511 | 452 |
| (II)-[Co([16]aneN$_4$)Cl$_2$]ClO$_4$ | 2341 | 1441 | 514 |
| (I)-[Co([16]aneN$_4$)Cl$_2$]ClO$_4$ | 2249 | 1457 | 452 |

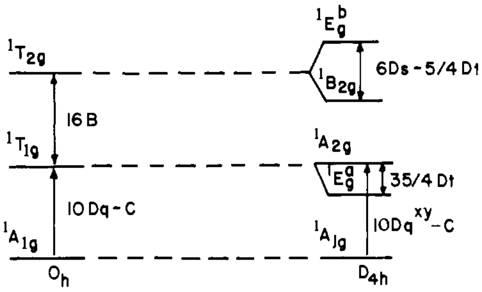

Figure 2. Energy level diagrams for a low-spin d$^6$ Ion in $O_h$ and $D_{4h}$ symmetry.

energy as do the $^1E_g{}^a$ and the composite $^1B_{2g} + {}^1E_g{}^b$ bands. In the case of the dibromo derivatives, charge transfer masks the ($^1B_{2g} + {}^1E_g{}^b$) $\leftarrow$ $^1A_{1g}$ transition and much of the $^1A_{2g} \leftarrow {}^1A_{1g}$ transition. Again, the shift to lower energy of the $^1E_g{}^a \leftarrow {}^1A_{1g}$ transition is observed as the size of the ring increases. All but one broad band is masked for the diazido, diisothiocyanato, and dinitro derivatives. Since these derivatives are possibly mixtures of isomers, as have been identified for the dichloro derivatives, the spectra cannot be interpreted in any detail. The broad unresolved band, if a composite of the $^1E_g{}^a$ and $^1A_{2g}$ transitions, reflects that the value of $Dq^z$ for these derivatives is closer to the value of $Dq^{xy}$ than is true for the Cl$^-$ and CN$^-$ complexes. Three bands are again observed for the dicyano complexes; this indicates that the $^1A_{2g}$ level has dropped in energy below the $^1E_g{}^a$ level because cyanide is a stronger ligand than is the macrocycle. Within each set of derivatives in Table V the observed bands move to lower energy as the macrocyclic ring becomes larger.

Examination of the calculated ligand field parameters in Table VI for *trans*-Co([13-16]aneN$_4$)Cl$_2$$^+$ complexes reveals several trends that are similar to those observed for the tetragonal Ni(II) and Fe(II) complexes of the same macrocyclic rings.[2,3] The $Dq^{xy}$ values are found to decrease as the ring size increases. These results confirm the spectrochemical series among the macrocycles:

$$[13]\text{aneN}_4 \gg [14]\text{aneN}_4 > [15]\text{aneN}_4 > [16]\text{aneN}_4$$

The $Dq^{xy}$ values of isomer II of *trans*-Co([15]aneN$_4$)Cl$_2$$^+$ and of *trans*-Co([16]aneN$_4$)Cl$_2$$^+$ are larger than those of their corresponding isomer I. From this it may be inferred that the effective ring size is different in the two isomers, with isomer II having the smaller effective ring size and exerting a stronger ligand field. Strain energy calculations on the isomers of *trans*-Co([15]aneN$_4$)Cl$_2$$^+$ (see below) have shown that the effective ring sizes of the two isomers are indeed different, with II being smaller than I.

**Electrochemistry of *cis*- and *trans*-[Co([12-16]aneN$_4$)Cl$_2$]ClO$_4$.** The half-wave potentials for the Co(III)/Co(II) couples are given in Table VII. The cyclic voltammograms for the *trans*-dichloro complexes indicate that the Co(III)/Co(II) reductions are not, in general, as reversible as those observed for a series of related *trans*-acetonitrile complexes.[18] The cathodic and anodic peaks are well defined, but the peak separations (~70 and 90 mV for [14]aneN$_4$ and [13]aneN$_4$, and ~150 mV for [15]- and [16]aneN$_4$, respectively) vary as a function of scan time. As well, the ratio of peak areas is slightly less than one, indicating that a slow chemical reaction may

**Table VII.** Half-Wave Potentials[a] for $[Co([13\text{-}16]aneN_4)Cl_2]^+$ in Acetonitrile[b]

| Ligand | $E_{1/2}$, V, $Co^{3+}/Co^{2+}$ | Peak separation,[c] mV |
|---|---|---|
| | Trans isomers | |
| $[13]aneN_4$ | −0.66 | 90 |
| $[14]aneN_4$ | −0.69 | 70 |
| $[15]aneN_4$ (I) | −0.38 | 93 |
| $[15]aneN_4$ (II) | −0.47 | 160 |
| $[16]aneN_4$ (I) | −0.15 | ~150 |
| $[16]aneN_4$ (II) | −0.11 | 150 |
| | Cis isomers | |
| $[12]aneN_4$ | −0.49 | 230 |
| $[13]aneN_4$ | −0.68 | 120 |
| $[14]aneN_4$ | −0.54 | 120 |

[a] Rotating platinum electrode, 600 rpm. [b] Vs. $Ag/AgNO_3$ (0.1 M) reference electrode, 0.1 M $t\text{-}Bu_4NBF_4$ as supporting electrolyte. [c] Scan rate, 500 mV $s^{-1}$, stationary platinum electrode.

**Table VIII.** $^{13}C$ NMR Data for *trans*-(I)-$[Co([15]aneN_4)Cl_2]^+$ and *trans*-(II)-$[Co([15]aneN_4)Cl_2]^+$

| Peak no. | Shift, ppm | Peak no. | Shift, ppm |
|---|---|---|---|
| | A. *trans*-(I)-$[Co([15]aneN_4)Cl_2]Cl$[a] | | |
| 1 | 53.0 | 6 | 48.0 |
| 2 | 52.7[b] | 7 | 44.6 |
| 3 | 51.9 | 8 | 26.0 |
| 4 | 51.2 | 9 | 25.1 |
| 5 | 49.3 | 10 | 21.4 |
| | B. *trans*-(II)-$[Co([15]aneN_4)Cl_2]Cl$[a] | | |
| 1 | 52.5 | 4 | 44.9 |
| 2 | 48.6 | 5 | 22.1[b] |
| 3 | 47.6 | | |

[a] In $D_2O$, 6 M DCl, ambient temperature, dioxane internal standard. Peak positions reported relative to $Me_4Si$ (dioxane resonance at 66.5 ppm relative to $Me_4Si$). [b] This absorption has approximately twice the intensity of any other band in the ligand spectrum (see ref 18).

follow the reduction process. Since it is evident that the [13]- and $[14]aneN_4$ derivatives are much better behaved at the r.p.e. than are the [15]- and $[16]aneN_4$ derivatives, we have investigated the difference further. ESR measurements at liquid nitrogen temperature made on the Co(II) derivatives obtained by controlled potential electrolysis of the respective Co(III) derivatives in acetonitrile containing tetra-*n*-butylammonium tetrafluoroborate indicate that the [13]- and $[14]aneN_4$ species are low spin, whereas the remaining species are high spin. It is not surprising to find that a change in spin state on reduction of Co(III) to Co(II) is accompanied by some enhanced degree of "irreversibility", but further study would be required in order to establish any cause and effect relationship. It should be noted that a change in spin state also occurs at the same point in the series for the analogous iron(II)[2] complexes. Further, such variations in the degree of reversibility of electrode processes have also been observed for other macrocyclic complexes of cobalt.[18]

Earlier studies have shown very clearly that the potential of the Co(III)/Co(II) couple is not sensitive, in general, to variations in the in-plane ligand field, while it is quite sensitive to variations in the axial ligand field. This is discussed elsewhere;[18] however, it has particular significance here because the half-wave potentials for the reductions of the complexes *trans*-$[Co([Z]aneN_4)Cl_2]^+$ show pronounced shifts with changes in macrocyclic ring size: $E_{1/2}$ varies in the series $[13] \geqslant [14] < [15] \ll [16]$. Thus $E_{1/2}$ changes only little (perhaps it increases slightly) on going from [13]- to $[14]aneN_4$, but a further increase in ring size substantially favors the formation of Co(II) ($E_{1/2}$ becomes less negative). The total range of $E_{1/2}$ is almost 600 mV. In contrast, earlier studies with complexes having 14-membered rings that varied in degree of unsaturation showed a total range for $E_{1/2}$ of only 250 mV with over half of that range being accounted for by only two compounds. The couple can generally be described as constant within an average deviation of about 50 mV, although $Dq^{xy}$ varies over some 14% of its total value. Examples are: $Me_4[14]$-1,3,8,10-tetraene$N_4$, $Dq^{xy}$ = 2960 $cm^{-1}$, $E_{1/2}$ = 0.12 V; $Me_6[14]$4,11-diene$N_4$, $Dq^{xy}$ = 2780 $cm^{-1}$, $E_{1/2}$ = 0.13 V; $Me_2[14]$1-ene$N_4$, $Dq^{xy}$ = 2720 $cm^{-1}$, $E_{1/2}$ = 0.08 V; $Me_6[14]aneN_4$, $Dq^{xy}$ = 2600 $cm^{-1}$, $E_{1/2}$ = 0.08 V. It follows that the systematic variation of $E_{1/2}$ for the Co(II)/Co(III) couple with ring size among the complexes reported here is novel and merits further consideration. The difference in $E_{1/2}$ values between the [14]- and $[16]aneN_4$ derivatives is ~0.55 V and is slightly larger than that observed, 0.30 V, for the analogous nickel complexes.[19] As will be considered below, the difference in half-wave potentials can be correlated with the release of strain energy upon reduction of the metal ion.

It is noted that the $E_{1/2}$ value for isomer I of *trans*-$Co([15]aneN_4)Cl_2^+$ is less negative than that for isomer II (−0.38 vs. −0.47 V), indicating that isomer I is easier to reduce than isomer II. This is consistent with the spectral results discussed previously and with the strain energy calculations (see below).

The $E_{1/2}$ value for reduction of *trans*-$Co([13]aneN_4)Cl_2^+$ appears, at first glance, to be anomalous. The same situation occurs for the analogous nickel complex.[19] The result reflects the well known stability of the 14-membered macrocyclic complexes of cobalt(III) as compared to the other ring size complexes. The apparent anomaly is interpreted below in terms of the strain energy of $Co([13]aneN_4)Cl_2^+$ being greater than that for $Co([14]aneN_4)Cl_2^+$ (see Table XII), so the release in strain energy upon reduction for $[13]aneN_4$ is greater than that for $[14]aneN_4$, thus stabilizing Co(II) relative to Co(III). The correlation of half-wave potentials with strain energy will be discussed more fully in a later section.

The electrochemical behavior of the *cis*-$Co([13\text{-}16]aneN_4)Cl_2^+$ complexes is also reported in Table VII. Like the analogous trans compounds, the complex containing the smallest ring system is not the hardest to reduce. $E_{1/2}$ is −0.68 V for *cis*-$Co([13]aneN_4)Cl_2^+$, while the 12-membered ring compound, which has $E_{1/2}$ = −0.49 V, is the easiest to reduce. The 14-membered ring complex exhibits an $E_{1/2}$ (−0.54 V) very similar to that of the 12-membered ring.

**Isomers of *trans*-$[Co([15]aneN_4)Cl_2]^+$.** The two isomers exhibit different colors, ligand field strengths, infrared spectra, electronic spectra, reduction potentials, $^{13}C$ NMR spectra, and solubilities. The chloride salt of isomer I is significantly more soluble in acetonitrile than is that of isomer II.

From data obtained on methanol solutions, isomer I gives $Dq^{xy}$ = 2303 $cm^{-1}$ and $Dq^z$ = 1511 $cm^{-1}$, while isomer II has its spectral bands all shifted to higher energies and gives $Dq^{xy}$ = 2421 $cm^{-1}$ and $Dq^z$ = 1465 $cm^{-1}$. Hence, the macrocyclic ligand exerts a stronger effect in isomer II. The electronic and infrared spectra prove that these two compounds both have the trans configuration. They are configurational isomers differing in the chiralities of the nitrogen atoms.

$^{13}C$ NMR data for the two isomers are shown in Figure 3 and Table VIII. Isomer I displays ten peaks. The intensity of the peak at 52.7 ppm is approximately twice that of the other bands, thus strongly suggesting that this spectral feature is due to the superposition of two resonances.[20] If this is so, then the 11 observed resonances correspond to 11 nonequivalent carbon atoms, indicating no symmetry in the molecule. The first seven absorptions (Table VIII) are assigned to the eight carbon

**Table IX.** Symmetries and Ring Conformations of Configurational Isomers of *trans*-[(Co[15]ane$N_4$)$Cl_2$]$^+$

| Isomer[a] | Point group | Chelate ring conformations[b] |
|---|---|---|
| a | $C_1$ | CCTg |
| b | $C_2$ | CTCg |
| c | $C_s$ | TCTp |
| d | $C_2$ | TTTg |
| e | $C_1$ | CTTp |
| f | $C_s$ | CCCp |

[a] See Figure 4. [b] T, twist; C, chair; g, gauche; p, eclipsed.

atoms adjacent to nitrogen atoms, while bands 8, 9, and 10 are assigned to the three remaining carbon atoms $\beta$ to nitrogen atoms in the ring. In contrast, isomer II gives only five peaks. Again the area of one of the peaks (22.1 ppm) suggests the presence of two unresolved resonances. Following the assignments for isomer I, peaks 1-4 are assigned to carbon atoms adjacent to nitrogen atoms, and peak 5 to a carbon atom $\beta$ to the nitrogen atoms. The number of observed peaks and the assignments are consistent with a molecule having either a mirror plane or a twofold axis passing through the cobalt atom and one carbon atom of a six-membered ring. Thus, isomer I belongs to the point group $C_1$, while isomer II is either $C_2$ or $C_s$.

Other differences between the two isomers aid in the deduction of their configurational structures. In methanol, the original green solution of isomer II gradually changes to a brown color, suggesting isomerization to a mixture of I and II. The percentage of each isomer at equilibrium in methanol has been calculated from their extinction coefficients at 520 and 420 nm. This gives 67 ± 3% of isomer I and 33 ± 3% of isomer II at 25 °C. The equilibrium constant for eq 5 is then calculated to be 2.

$$\text{isomer II} \underset{\text{methanol}}{\overset{K_{eq}}{\rightleftharpoons}} \text{isomer I} \qquad (5)$$

Isomer I can be converted to isomer II by reaction with lithium carbonate followed by acidifying with concentrated HCl.

$$\text{isomer I (brown)} \xrightarrow[\Delta,\ H_2O]{Li_2CO_3} \text{violet} \xrightarrow{\text{conc HCl}} \text{isomer II (green)} \qquad (6)$$

We note with interest that the isomer that is slightly favored thermodynamically (isomer I) exerts the weaker in-plane ligand field strength (2303 vs. 2421 $cm^{-1}$ for isomer II).

Since I and II are configurational isomers, they most probably differ in the orientation of the hydrogens on their secondary amine groups with respect to the metal-nitrogen plane. In theory, six basic forms are possible for the conformers (Figure 4) on the basis of these N-H orientations. The "+" and "−" signs represent hydrogens above, "+", or below, "−", the metal-nitrogen plane, respectively. The numbers are the numbers of carbons in the chelate rings. Table IX lists these possible stereoisomers of *trans*-Co([15]ane$N_4$)$Cl_2^+$ along with their point groups and chelate ring conformations. The conformations of six-membered chelate rings are indicated by either T (for twist) or C (for chair), while g (for gauche) and p (eclipsed) refer to the five-membered chelate ring. It is well known that the chair form is the most stable conformation for the six-membered ring,[21] while the gauche form is the one preferred for five-membered rings.

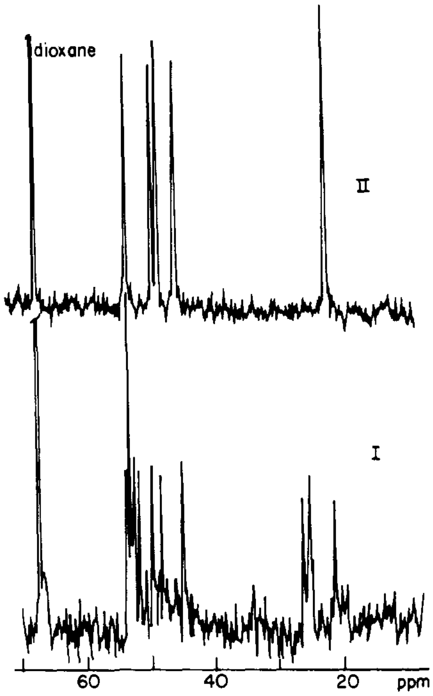

**Figure 3.** $^{13}C$ NMR spectra of the configurational isomers of *trans*-Co([15]ane$N_4$)$Cl_2^+$ (6 M DCl).

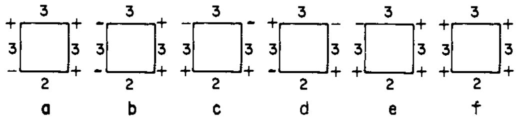

**Figure 4.** Possible configurational isomers for [15]ane$N_4$ in *trans*-Co([15]ane$N_4$)$Cl_2^+$.

The minimized conformational strain energies were calculated for isomers a through f using the method previously described by DeHayes and Busch.[22] The results are shown in Table X, where $R$ is the enthalpy arising from bond length deformations, NB from non-bonded interactions, $\theta$ from bond angle deformations, and $\phi$ from torsional angle deformations. $H$ is the total strain enthalpy and $G$ is the total strain free energy calculated from $H$ and the classical statistical mechanical entropy.[22] It is important to note that the calculated thermodynamic values are relative, not to be compared with free energies of formation, etc.

**Table X.** Calculated Conformation Energies for Configurational Isomers of *trans*-[Co([15]ane$N_4$)$Cl_2$]$^+$ (in kcal/mol)

| Isomer[a] | $R$ | NB | $\theta$ | $\phi$ | $H$ | $G$ |
|---|---|---|---|---|---|---|
| a | 4.26 | 5.32 | 8.02 | 3.73 | 21.33 | −18.27 |
| b | 4.52 | 6.26 | 8.69 | 3.36 | 22.83 | −16.40 |
| c | 3.25 | 7.24 | 8.86 | 6.05 | 25.40 | −13.99 |
| d | 3.52 | 7.63 | 7.64 | 6.67 | 25.47 | −12.90 |
| e | 3.71 | 9.39 | 11.82 | 5.05 | 29.97 | −8.29 |
| f | 4.30 | 8.20 | 12.50 | 5.47 | 30.46 | −8.19 |

[a] See Figure 4.

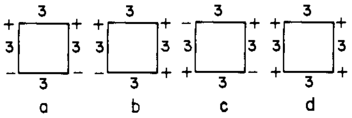

Figure 5. Possible configurational isomers for [16]ane$N_4$ in *trans*-Co([16]ane$N_4$)$Cl_2^+$.

Isomers a through f are listed in Table X in the order of increasing strain energy, which is the order of decreasing stability. The most stable isomer exhibits no symmetry (point group $C_1$, Table IX) and therefore 11 peaks would be expected in its $^{13}C$ NMR spectrum. Of the observed two isomers, I is the more stable and displays no symmetry in the $^{13}C$ NMR spectrum; hence, isomer I is assigned configuration a. Isomer II is less stable than isomer I and its $^{13}C$ NMR shows either $C_2$ or $C_s$ symmetry. In addition, isomer II can be prepared directly from *cis*-Co([15]ane$N_4$)$CO_3^+$ by addition of HCl. The fact that there is no N-H bond rupture during this process is shown by the lack of exchange of NH for ND in a reaction run in $D_2O$/DCl. Hence, the configuration for isomer II is the same as that for the corresponding *cis*-carbonato complex. This fact further limits the range of choice of configurations for isomer II, since only those configurations which have two diagonal hydrogens on the same side of the macrocyclic plane can fold into the cis conformation.[23] On this basis, configurations a, d, e, and f are acceptable choices. Consideration of the symmetry shown in the $^{13}C$ NMR spectrum limits the choice to d and f. Finally, in view of the strain energy results structure d is the predicted configuration for isomer II.

An earlier preliminary report[5] from these laboratories, introduced the concept of an ideal metal donor distance (M-N) for square planar nickel complexes. This ideal distance is predicted by setting the metal-nitrogen stretching force constant to zero and allowing the ring to relax to its "ideal" size. (Present calculations differ from earlier ones in that the trans axial chlorides are included here.) Analogous calculations for the ideal ring size for configurations a and d for [Co([15]ane$N_4$)$Cl_2$]$^+$ yield the values 2.28 and 2.23 Å, respectively. The metal-nitrogen distances in the energy minimized structures, but with M-N force constants included, are 2.08 and 2.07 Å, respectively. Thus, the macrocycle in d is expected to exert a stronger ligand field than does a. This prediction is in accordance with the relative $Dq^{xy}$ values of Table VI where it is seen that the value for isomer II (d) is larger than that for isomer I (a). The relative oxidation potentials are also consistent with this conclusion, since II is more difficult to reduce than I.

**The Isomers of *trans*-[Co([16]ane$N_4$)$Cl_2$]$ClO_4$.** Metathesis of the bromochloro complex (Experimental Section) of [16]ane$N_4$ with lithium chloride in hot methanol gives two crops of crystals. A green material precipitates from the cooled solution and a brown compound is obtained by reducing the volume of the filtrate. In acetonitrile, isomer I (brown compound) displays calculated $Dq$ values of 2249 $cm^{-1}$ for the macrocyclic ligand and 1457 $cm^{-1}$ for the axial ligands (chloride). Isomer II (green) is characterized by $Dq^{xy}$ = 2341 $cm^{-1}$ and $Dq^z$ = 1441 $cm^{-1}$. The stronger in-plane ligand field is accompanied by a weaker axial ligand field.

Isomer II, like isomer II of *trans*-Co([15]ane$N_4$)$Cl_2^+$, could be obtained by acidifying the *cis*-carbonato compound. In methanol, isomer II slowly isomerizes to a mixture of isomer I and II. However, due to the sparing solubility of isomer II in methanol, the absorptivity of this compound has not been obtained. Hence, it is not possible to calculate the percentage of each isomer at equilibrium, nor to calculate the equilibrium constant.

Attempts to investigate the isomerization to isomer I in water failed because of the easy reduction of the cobalt(III) in the diaquo complex to cobalt(II). This is not surprising, since the half-wave potential for the Co(III)/Co(II) couple of *trans*-[Co([16]ane$N_4$)$Cl_2$]$ClO_4$ is −0.15 V in acetonitrile. Of the macrocyclic cobalt(III) complexes investigated, the 16-membered ring complexes are the easiest to reduce.

Table XI. Calculated Conformational Energies of Some Possible *trans*-[Co([16]ane$N_4$)$Cl_2$]$^+$ Isomers (in kcal/mol)

| Isomer[a] | $R$ | NB | $\theta$ | $\phi$ | $H$ |
|---|---|---|---|---|---|
| a | 7.81 | 10.18 | 10.98 | 6.60 | 35.56 |
| b | 6.26 | 10.36 | 13.87 | 6.09 | 36.57 |

[a] See Figure 5. Attempts to calculate strain energies of other isomers of [16]ane$N_4$ complexes were unsuccessful due to very high strain energies of these structures.

The configurations of the isomers have been assigned, tentatively, on the basis of models and conformational energy considerations. The possible conformers for the [16]ane$N_4$ derivatives reduce to four forms because of the equal numbers of carbon atoms in the chelate rings (Figure 5). Of the four conformers, forms a and b both have two twist and two chair conformations for the chelate rings. It is likely that one of these two is the least strained. The results of conformational energy calculations are shown in Table XI. The strain energy of conformer a is less than that of conformer b, but the two values are rather close. Consequently, isomer I is tentatively assigned configuration a, which has the same N-H configurations as the lowest energy form of the [14]ane$N_4$ ring. Isomer II has a pair of diagonal hydrogen atoms on the same side of the metal nitrogen plane, hence its ability to fold. Therefore, isomer II is tentatively assigned configuration b, the lowest energy form with diagonal hydrogen atoms.

Only one isomer of *trans*-[Co([13]ane$N_4$)$Cl_2$]Cl was isolated and this compound displays five peaks in its $^{13}C$ NMR spectrum (6 M DCl), thus indicating a symmetrical structure. The configuration having the least strain energy has two hydrogen atoms on the six-membered ring on the same side of the metal-nitrogen plane and the other two hydrogens atoms on the opposite side of the metal-nitrogen plane. This structure is consistent with the observed $^{13}C$ NMR spectrum, and, therefore, is tentatively assigned as the structure of *trans*-[(Co[13]ane$N_4$)$Cl_2$]Cl. Only one isomer[24] of *trans*-[Co([14]ane$N_4$)$Cl_2$]$^+$ is isolated by addition of the amine ligand to an appropriate cobalt(II) salt followed by air oxidation.[7]

**Ring Size Effects.** The value of $Dq^{xy}$ reported by Wentworth and Piper[6] for the ethylenediamine in *trans*-diacidobisethylenediamine complexes of cobalt(III) is 2530 $cm^{-1}$, and that value is accepted as normal for saturated nitrogen bases for the purposes of the discussion that follows. Because of the fortuitous occurrence of the configurational isomers of [15]ane$N_4$ and [16]ane$N_4$ in their trans complexes, we have six complexes of the general formula *trans*-Co([13-16]ane$N_4$)$Cl_2^+$ whose properties can be examined in detail for ring size correlations. Calculations show that strain energies (Table XII) for the various macrocycles bound to $Co^{3+}$ vary in the sequence: II-[16]ane$N_4$ $\gtrsim$ I-[16]ane$N_4$ $\gg$ II-[15]ane$N_4$ > I-[15]ane$N_4$ $\gg$ [14]ane$N_4$ $\ll$ [13]ane$N_4$. Because of its nature, the effects of strain energy relate to stability and it is not surprising that qualitative observations suggest that stabilities do indeed vary in this approximate sequence (see earlier discussion of properties).

A revealing relationship exists between the ligand field strength for the macrocycle in *trans*-Co([13-16]ane$N_4$)$Cl_2^+$ and the deviation of the *ideal M-N distance* from the *best fit* value. We have attempted to calculate the "ideal" metal-nitrogen distance which each macrocycle would assume in the

**Table XII.** Strain Energies and Ideal M-N Distances for $[Co([X]\text{-}aneN_4)Cl_2]^+$ Complexes[a]

| Ligand (isomer) | Strain energy, kcal | Ideal M-N, Å | Δ(M-N) |
|---|---|---|---|
| [13]ane$N_4$ | 19.74 | 2.01 | −0.12 |
| [14]ane$N_4$ | 11.53 | 2.13 | 0.00 |
| [15]ane$N_4$ (I) | 21.33 | 2.28 | 0.15 |
| [15]ane$N_4$ (II) | 25.47 | 2.23 | 0.10 |
| [16]ane$N_4$ (I) | 35.56 | 2.42 | 0.29 |
| [16]ane$N_4$ (II) | 36.57 | *b* | *b* |

[a] Δ(M-N) is the difference between the ideal M-N distance and the "best fit" ideal M-N distance for [14]ane$N_4$. [b] These values are unavailable for [16]ane$N_4$ (II) due to the large distortions from planarity, which result from setting the metal-nitrogen stretch force constant equal to zero.

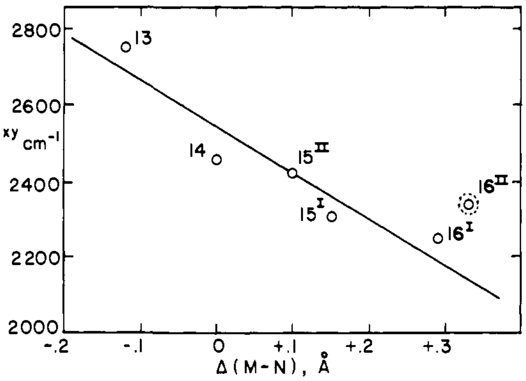

Figure 6. Correlation of $Dq^{xy}$ for the *trans*-Co([13-16]ane$N_4$)$Cl_2^+$ complexes with variation of the ideal M-N distance from the best fit value (line shown is least-squares fit).

absence of the restrictive effects of coordination, but with retention of the relatively planar conformation of the macrocylic ring. In order to do this we began with the coordinates of the strain energy minimized structure of the *trans*-Co([13-16]-ane$N_4$)$Cl_2^+$ complex. The metal-nitrogen stretching force constants were then set to 0.0, while all other interactions were retained and the minimization calculation was performed. The average metal-nitrogen distance of the resulting structure represents the hole size for which the strain energy of the ligand is a minimum; this is the "ideal" M-N distance. Coordination to a metal ion which is either larger or smaller than this ideal size results in an increase in the strain energy of the ligand. Since [14]ane$N_4$ is judged to fit $Co^{3+}$ with relatively little stress on the $Co^{3+}$-N linkage, the calculated *ideal M-N* (Table XII) of 2.13 Å is taken as a parameter reflecting that good fit.[25] The nonfit of the other rings (in their specific configurations) can then be judged by the differences between the calculated ideal M-N values and the best fit value of 2.13 Å. The resulting Δ(M-N) values are graphed against $Dq^{xy}$ in Figure 6. The correlation is rather good with a correlation coefficient of 0.94.

The variation in $Dq^{xy}$ among the configurational isomers for [15]ane$N_4$ and [16]ane$N_4$ involves an additional relationship. In both cases, the more strained isomer exhibits the smaller ideal M-N distance and the greater $Dq^{xy}$. The greater $Dq^{xy}$, in turn, more closely approaches a normal value for four nitrogens bound to $Co^{3+}$. The latter result is consistent with the fact that these rings are both oversized for that metal ion, so that decreasing the metal ion site causes it to change in the direction of the ideal M-N distance. This suggests a model in which a more strained configuration for these rings is derived from the less strained one by some internal twist in the ring that serves to make it smaller. This, of course, is not a complete misrepresentation of the change in the ring that accompanies the inversion in chirality of one or more of the bound amines of the macrocycle (i.e., the change that transforms one configurational isomer into another).

It is important to emphasize the fact that the changes in ligand field strengths ($Dq^{xy}$) of the complexes *trans*-Co([13-16]ane$N_4$)$Cl_2^+$ do not correlate with strain energy. $Dq^{xy}$ increases in the series [16](I) < [16](II) < [15](I) < [15](II) < [14] < [13], while the strain energy changes in the sequence [16](II) > [16](I) > [15](II) > [15](I) > [14] < [13]. Thus $Dq^{xy}$ responds to the misfit between the metal ion and the metal ion site in the ring rather than the total strain energy associated with coordination.

These results clearly demonstrate the effect of ring size on the ligand field strengths of donor atoms in complexes with macrocyclic ligands. Although a good correspondence between the normal metal-donor distance and the most favorable hole size for a given macrocyclic ligand facilitates binding with normal ligand field interactions, poor fits between the ring and the included metal ion lead to alterations in the metal-donor linkage. The effect may be large when the fit is very poor. Thus, the ligand field strength may be greatly increased or decreased by macrocycles that fit the metal ion very poorly. Although we have demonstrated the phenomenon using macrocycles chelated in a coplanar fashion about the metal ion, there is no reason why this should be the only geometry wherein such effects might occur. The resulting general conclusion that metal donor interactions may be controlled stereochemically has broad significance. For example, the rather vaguely formulated *entatic* effect of Vallee and Williams[29] could be rationalized in these terms.

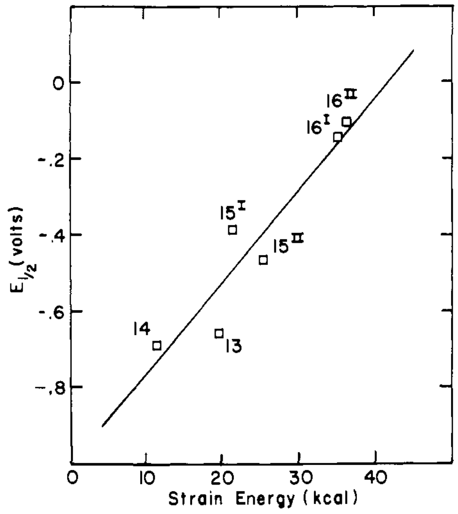

Figure 7. Correlation of half-wave potentials for the $Co^{2+}/Co^{3+}$ couple with the minimized strain energy for *trans*-Co([13-16]ane$N_4$)$Cl_2^+$ complexes (line shown is least-squares fit).

The electrochemical data of Table VII correlate well with the variations in strain energy as shown in the graph in Figure 7. The data form a good linear correlation having a least-squares correlation coefficient $r^2$ of 0.88. Thus $Co^{3+}$ is favored over $Co^{2+}$ as the strain energy decreases. The fact of the correlation is evident, but whether or not it is meaningful will require the test of time. The nature of the correlation must be viewed as unusual. The nature of an electrochemical change is being compared with a theoretical ground state property of the pure reactant in the gas phase. This suggests that the structural parameter responsible for the variations in $E_{1/2}$ that have been observed is purely that of the reactant ($Co^{III}([Z]\text{-}aneN_4)Cl_2^+$) and that the corresponding parameter for the product ($Co^{II}([Z]aneN_4)Cl_2^0$) is quite unimportant. Of most interest is the implication that the property (strain energy) of the product (Co(II) complex) is unimportant. This suggests that the strain energies of the various macrocycles bound to the product are either all about the same or small compared to other energies that relate to the system. An obvious model follows from this, but it is not without its difficulties. Since rates correlate with the strain energies of the reactants, the products must involve structures in which the strain energies are largely relieved. Thus it is suggested that upon reduction of the central metal ion (from $Co^{3+}$ to $Co^{2+}$) the ligand is relatively free to relax into a less strained mode of chelation. This is consistent with the general lability of $Co^{2+}$ complexes as compared to $Co^{3+}$ complexes. The nature of such relaxations might vary from ring size to ring size. For example, the small 13-membered ring would require expulsion, to some extent, of the larger (than $Co^{3+}$) $Co^{2+}$ ion from within the ring. Obviously the relief of strain for the oversized rings could follow a different course. From the behavior of $Ni^{2+}$ it might be expected[30] that the 15-membered ring would simply fit $Co^{2+}$ better than $Co^{3+}$.

## Experimental Section

**Physical Measurements.** Perkin-Elmer 337 or 457 spectrophotometers were employed to record infrared spectra. The samples were prepared as Nujol mulls or KBr pellets. Visible absorption spectra were obtained with a Cary Model 14R spectrophotometer. The spectra were subjected to Gaussian analysis where appropriate. $^{13}C$ NMR spectra were obtained on a Bruker HX-90 spectrometer at 22.625 MHz with internal deuterium lock and using broad band decoupling. Peak positions were reported relative to $Me_4Si$ by assuming the dioxane peak in $D_2O$ occurs at 66.5 ppm relative to $Me_4Si$. Conductivity measurements were performed with an Industrial Instruments Model RC16B conductivity bridge on $\sim 10^{-3}$ M solutions at room temperature. Solid-state magnetic moments were determined under 35 Torr of helium gas using the Faraday method.[31] Diamagnetic corrections were made using Pascal's constants.[32] Elemental analyses were performed by Chemalytics, Inc., Galbraith Laboratories, and Dr. Wayne Schammel of this laboratory. Electrochemical measurements in high purity acetonitrile were carried out in a Vacuum Atmospheres Dritrain under nitrogen as previously described.[19]

**Ligands.** The ligands [13]ane$N_4$, [15]ane$N_4$, and [16]ane$N_4$ were prepared by published procedures[2,3] as was *trans*-[Co([14]ane$N_4$)$Cl_2$]Cl.[7]

***cis*- and *trans*-[Co([13]ane$N_4$)$Cl_2$]Cl.** Cobalt(II) chloride hexahydrate (1.0 g, 4.2 mmol) and a slight excess of [13]ane$N_4$ (0.8 g) were warmed in 60 mL of methanol for 10 min. HCl was added dropwise to the solution until the red-brown solution turned green (about 1 mL). Air was then bubbled through the solution for 2 h and the volume of solution was reduced to 25 mL. At this point green crystals separated which were recrystallized from methanol. Further reduction of the volume of the original filtrate resulted in isolation of the red cis complex. The perchlorate salt was obtained by adding several drops of perchloric acid to the reaction mixture.

***cis*- and *trans*-[Co([13]ane$N_4$)$Br_2$]$ClO_4$.** These compounds were prepared in the same fashion as above except that 48% HBr was used.

***trans*-[Co([13]ane$N_4$)$(N_3)_2$]$ClO_4$, *trans*-[Co([13]ane$N_4$)$(NCS)_2$]$ClO_4$, *trans*-[Co([13]ane$N_4$)$(NO_2)_2$]$ClO_4$, and *trans*-[Co([13]ane$N_4$)$(CN)_2$]$ClO_4$.** Metathesis of the *trans*-dichloro complex with the appropriate lithium or sodium salt (2:1 ratio) in hot methanol resulted in the separation of the above derivatives upon cooling. All these derivatives were recrystallized from hot methanol except for the dicyano derivative, which was recrystallized from hot water.

***trans*-[Co([15]ane$N_4$)$Cl_2$]$ClO_4$ and *trans*-[Co([15]ane$N_4$)$Br_2$]$ClO_4$.** The same procedures were applied to these complexes as were used for the corresponding [13]ane$N_4$ derivatives.

***trans*-[Co([15]ane$N_4$)$(N_3)_2$]$ClO_4$, *trans*-[Co([15]ane$N_4$)$(NCS)_2$]$ClO_4$, *trans*-[Co([15]ane$N_4$)$(NO_2)_2$]$ClO_4$, and *trans*-[Co([15]ane$N_4$)$(CN)_2$]$ClO_4$.** These complexes were prepared by metatheses from the parent dichloro complexes as described for the [13]ane$N_4$ complexes. Methanol was used to recrystallize these complexes, except the cyanide derivative for which water was used.

**Isolation of the Isomers (I and II) of *trans*-Co([15]ane$N_4$)$Cl_2^+$. Isomer I.** The perchlorate salt of the dichloro derivative obtained by the procedure stated above was recrystallized from acetonitrile and water. At this point, the product was about 95% pure isomer I (brown in color). The brown perchlorate salt was dissolved in acetonitrile and passed through a Dowex 1X8 200–400 mesh anion exchange column ($Cl^-$ form) at a rate of 10 s/drop. The eluent was concentrated by rotary evaporation. Some green solid (isomer II) precipitated. This was filtered and the volume of the filtrate was further reduced in order to isolate isomer I (tan) as the chloride salt. The tan chloride salt was dissolved in methanol and $NH_4NO_3$ was added to produce crystals of the nitrate salt.

**Isomer II.** *trans*-[Co([15]ane$N_4$)$Cl_2$]$ClO_4$ was dissolved in acetonitrile containing several milliliters of water, and warmed with $Li_2CO_3$ with stirring for 2 h. The solution color turned violet. The excess $Li_2CO_3$ was removed by filtration. HCl was added dropwise (2 mL) and the solution was warmed for 30 min. At this time the color had changed to green. The solid product, which was mainly green isomer, was dissolved in acetonitrile and passed through a Dowex 1X8 (200–400 mesh) anion exchange column ($Cl^-$ form). The chloride salt of isomer II (green) was obtained by reducing the volume of the eluent. The nitrate salt could be obtained in the same way as described for isomer I.

***trans*-[Co([16]ane$N_4$)$Br_2$]$ClO_4$.** To a methanol solution of [16]ane$N_4$ (0.5 g, 50 mL) was added 0.48 g of anhydrous $CoBr_2$. The resulting magenta solution was warmed for 20 min, a slight excess of $LiClO_4$ was added, and the solution was warmed for another 10 min. The methanol was removed by evaporation and the solid was redissolved in chloroform and the solution was filtered. Evaporation followed by dissolution in chloroform was repeated once more. $Br_2$ was then added dropwise to the chloroform solution until the magenta color was completely gone (several drops) and was replaced by an amber-colored solution from which [Co([16]ane$N_4$)$Br_2$]$ClO_4$ precipitated. The product was filtered, washed with chloroform, and recrystallized from hot methanol.

***trans*-[Co([16]ane$N_4$)$(N_3)_2$]$ClO_4$, *trans*-[Co([16]ane$N_4$)$(NCS)_2$]$ClO_4$, *trans*-[Co([16]ane$N_4$)$(NO_2)_2$]$ClO_4$, and *trans*-[Co([16]ane$N_4$)$(CN)_2$]$ClO_4$.** Metathesis of the dibromo derivative with the appropriate lithium or sodium salt in hot methanol resulted in the above derivatives. All were recrystallized from hot methanol to which a few drops of perchloric acid had been added.

***trans*-[Co([16]ane$N_4$)$Cl_2$]$ClO_4$ (isomers I and II).** *trans*-[Co([16]ane$N_4$)$Cl_2$]$ClO_4$ was synthesized in the same way as for the dibromo derivative except the product after the $Br_2$ oxidation was [Co([16]ane$N_4$)BrCl]$ClO_4$, and this was dissolved in hot methanol to which a slight excess of LiCl was added. Green isomer II was obtained from the cooled solution. Brown isomer I was obtained by reducing the volume of the filtrate. Both were recrystallized from methanol and acetonitrile.

**Acknowledgment.** We would like to thank Dr. Charles Cottrell for obtaining the $^{13}C$ NMR spectra. The support of this research program by the National Science Foundation and by Grant No. GM 10040 from the National Institute of General Medical Sciences of the U.S. Public Health Service is gratefully acknowledged.

## References and Notes

(1) L. F. Lindoy and D. H. Busch, *Prep. Inorg. React.*, Vol. **6**, 1 (1971).
(2) D. D. Watkins, Jr., D. P. Riley, J. A. Stone, and D. H. Busch, *Inorg. Chem.*, **15**, 387 (1976).
(3) L. Y. Martin, Ph.D. Thesis, The Ohio State University, 1974.
(4) D. H. Busch, K. Farmery, V. Goedken, V. Katovic, A. C. Melnyk, C. R. Sperati, and N. Tokel, *Adv. Chem. Ser.*, **No. 100**, 44 (1971).
(5) L. Y. Martin, L. J. DeHayes, L. J. Zompa, and D. H. Busch, *J. Am. Chem. Soc.*, **96**, 4046 (1974).
(6) R. A. D. Wentworth and T. S. Piper, *Inorg. Chem.*, **4**, 709, 1524 (1965).
(7) B. Bosnich, C. K. Poon, and M. L. Tobe, *Inorg. Chem.*, **4**, 1102 (1965).
(8) C. K. Poon and M. L. Tobe, *J. Chem. Soc. A*, 2069 (1967).
(9) C. K. Poon and M. L. Tobe, *J. Chem. Soc. A*, 1549 (1968).
(10) J. P. Collman and P. W. Schneider, *Inorg. Chem.*, **5**, 1380 (1966).
(11) W. J. Geary, *Coord. Chem. Rev.*, 7, 81 (1971).
(12) C. K. Poon, *Inorg. Chim. Acta*, **5**, 322 (1971).
(13) K. Nakamoto, "Infrared Spectra of Inorganic and Coordination Compounds", Wiley, New York, N.Y., 1963.
(14) A. B. P. Lever, "Inorganic Electronic Spectroscopy", Elsevier, New York, N.Y., 1968, p 306.
(15) R. B. Penland, T. J. Lane, and J. V. Quagliano, *J. Am. Chem. Soc.*, **78**, 887 (1956).
(16) D. M. L. Goodgame and M. A. Hitchman, *Inorg. Chem.*, **5**, 1303 (1966).
(17) S. C. Jackels, K. Farmery, E. K. Barefield, N. J. Rose, and D. H. Busch, *Inorg. Chem.*, **11**, 2893 (1972).
(18) A. M. Tait, F. V. Lovecchio, and D. H. Busch, *Inorg. Chem.*, in press, and references cited therein.

(19) F. V. Lovecchio, E. S. Gore, and D. H. Busch, *J. Am. Chem. Soc.*, **96**, 3109 (1974).

(20) The residual paramagnetism observed for these complexes may provide a common spin-lattice relaxation mechanism, resulting in near equal $T_1$ values for all the carbon atoms. This makes a comparison of band intensities meaningful.

(21) C. J. Hawkins, "Absolute Configuration of Metal Complexes", Wiley-Interscience, New York, N.Y., 1971.

(22) L. J. DeHayes and D. H. Busch, *Inorg. Chem.*, **12**, 1505, 2010 (1973).

(23) L. G. Warner and D. H. Busch, *J. Am. Chem. Soc.*, **91**, 4092 (1969).

(24) We are grateful to a referee who pointed out that a second isomer of *trans*-[Co([14]aneN$_4$)Cl$_2$]$^+$ has been prepared by reaction with HCl of the (+)$_{546}$-*cis*-oxalato complex.[26] Referring to Figure 4, and replacing the uppermost three-carbon linkage with a two-carbon linkage, the possible trans isomers of [14]aneN$_4$ can be designated by structures b through f. Calculations for these isomers of *trans*-[Co([14]aneN$_4$)Cl$_2$]$^+$ result in total strain energy values of 11.53 (b), 27.78 (c), 19.51 (d), 20.47 (e), and 20.04 kcal (f), respectively. The isomer initially prepared by Bosnich et al.[7] is assigned the lowest energy structure (b) analogous to the known structure[27] of the [Ni([14]aneN$_4$)Cl$_2$] complex. Structure d has been assigned to the isomer resulting from decomposition of the *cis*-oxalato complex.[26] It should be noted that *cis*-[Co([14]aneN$_4$)Cl$_2$]$^+$ has been shown by x-ray crystallography[28] to have N-H configurations corresponding to isomer d of the *trans*-dichloro derivative. For structures b and d we calculate ideal metal-nitrogen distances of 2.13 and 2.11 Å, respectively. Thus we would predict very similar values of $Dq^{xy}$ for these two trans isomers, and indeed the observed spectra support this prediction.

(25) The M-N distances of Table XII are not expected to be accurate in the absolute sense; however, the differences between them are believed to have significance. Consequently, it is preferable to consider *ideal M-N* as a parameter reflecting the fit or nonfit of a given metal ion to the ring. Alternately, one could arbitrarily seek to add or subtract an increment that would bring this parameter into coincidence with experiment for the best fit case. We have chosen not to use this alternate procedure.

(26) J. Cragel, Jr., and B. E. Douglas, *Inorg. Chim. Acta*, **10**, 33 (1974).

(27) B. Bosnich, R. Mason, P. J. Pauling, G. B. Robertson, and M. L. Tobe, *Chem. Commun.*, 97 (1965).

(28) R. Mason, G. B. Robertson, and P. O. Whimp, unpublished results.

(29) B. L. Vallee and R. J. P. Williams, *Proc. Natl. Acad. Sci. U.S.A.*, **59**, 498 (1968).

(30) L. Y. Martin, C. R. Sperati, and D. H. Busch, *J. Am. Chem. Soc.*, in press.

(31) V. Katovic, L. F. Lindoy, and D. H. Busch, *J. Chem. Educ.*, **49**, 117 (1972).

(32) R. E. Mabbs and D. J. Machin, "Magnetism and Transition Metal Complexes", Chapman and Hall, London, 1973, p 5.

---

# Near-Zero-Coordinate Thallium(I). The Crystal Structures of Hydrated and Dehydrated Zeolite A Fully Exchanged with TlOH

**Roger L. Firor and Karl Seff***

*Contribution from the Chemistry Department, University of Hawaii, Honolulu, Hawaii 96822.*

*Received November 1, 1976*

**Abstract:** The crystal structures of vacuum-dehydrated ($a$ = 12.180 (2) Å) and hydrated ($a$ = 12.380 (2) Å) zeolite A which had been fully exchanged with aqueous TlOH have been determined by single-crystal x-ray diffraction techniques in the cubic space group $Pm3m$. The structures were refined to final $R$ (weighted) indices of 0.057 and 0.062, respectively. In the dehydrated structure, six equivalent Tl$^+$ ions lie on threefold axes in the large cavity opposite 6-oxygen rings, and three other Tl$^+$ ions occupy an equipoint in the planes of the oxygen 8-rings. In the sodalite unit, two equivalent Tl$^+$ ions are located on a common threefold axis near 6-rings on opposite sides of the origin. *The twelfth Tl$^+$ ion occupies a unique and unusual position in the large cavity, on a mirror plane and off a threefold axis, 3.21 Å from the nearest framework oxide ion. This Tl$^+$ ion is approximately 0.42 Å farther from its nearest neighbor than the sum of the ionic radii would indicate.* This situation has occurred because insufficient sites are available on the inner surface of the zeolite to accommodate all of the large cations present—by difference, one Tl$^+$ ion per unit cell must occupy a site where it can interact only weakly with the framework, its only possible ligand. In the hydrated structure, 13 Tl$^+$ ions are present. Seven occupy threefold axis sites opposite 6-rings in the large cavity, approximately 1.5 Å from the O(3) planes, while three Tl$^+$ ions are located in the planes of the 8-rings as in the dehydrated structure. In the sodalite unit, the remaining three Tl$^+$ ions form a nearly equilateral triangle, and are bridged, it is presumed, by a hydroxide ion which entered the zeolite from the TlOH exchange solution. Nine water molecules per unit cell have been located: three bridge between the Tl$^+$ ions opposite 6-rings in the large cavity, and the remaining six are associated with the three Tl$^+$ ions in the 8-oxygen rings.

Zero-coordinate cations,[1-4] or severely under-coordinated cations (this work), can be prepared by the ion-exchange of large monovalent cations into zeolite A followed by vacuum dehydration. Such unusual coordination occurs because all of the sites available to large cations at the zeolite framework are filled before all of the anionic charges of the framework are balanced, leaving some cations uncoordinated. Reference 2 discusses in some detail the conditions necessary for zero-coordinate cations to exist in zeolite A.

Three examples of zero-coordinate cations are known. In dehydrated K$_{12}$-A,[1,5] one K$^+$ ion per unit cell is located deep within the large cavity, 4.25 Å from its nearest neighbors, three oxide ions of a 6-oxygen ring.[6] In dehydrated Rb$_{11}$Na$_1$-A,[2,3,5] a Rb$^+$ ion occupies a similar position at distances of 4.35 Å. In dehydrated Cs$_7$K$_5$-A,[4,5] a K$^+$ ion is 4.40 Å from the same nearest neighbors. These monovalent cations can be considered zero-coordinate because their closest approaches to framework oxide ions are long, in comparison to the sum of the appropriate ionic radii, by 1.6–1.75 Å.[7]

This work was undertaken in the hope of preparing fully Tl$^+$-exchanged dehydrated zeolite A, which should contain an under-coordinate, possibly zero-coordinate, Tl$^+$ ion. This expectation was based on the previously determined structure of dehydrated Rb$_{11}$Na$_1$-A[2,3]—the ionic radius of Tl$^+$ (1.47 Å)[7] is the same as that of Rb$^+$. It was also suspected that dehydrated Tl$_{12}$-A might be different from dehydrated Rb$_{11}$Na$_1$-A[2,3] and K$_{12}$-A[1] because of the greater covalency of Tl$^+$.

The crystal structures of hydrated and dehydrated Tl$^+$-exchanged zeolite A have been studied before. In 1971, Riley, Seff, and Shoemaker determined the crystal structures of hydrated and dehydrated Tl$_{11}$-A;[8] more recently and less accurately, the hydrated structure was redetermined by Thöni[9] who was able to locate only ten Tl$^+$ ions per unit cell. The